HHS Public Access

Author manuscript

Drug Dev Ind Pharm. Author manuscript; available in PMC 2018 August 01.

Published in final edited form as:

Drug Dev Ind Pharm. 2017 February ; 43(2): 264–274. doi:10.1080/03639045.2016.1236811.

Modified Release Itraconazole Amorphous Solid Dispersion to Treat *Aspergillus fumigatus*: Importance of the Animal Model Selection

Julien Maincent[1], **Laura K. Najvar**[2], **William R. Kirkpatrick**[2], **Siyuan Huang**[1], **Thomas F. Patterson**[2], **Nathan P. Wiederhold**[2], **Jay I. Peters**[2], and **Robert O. Williams III**[1,*]

[1]College of Pharmacy, The University of Texas at Austin, Austin, TX 78712, USA

[2]University of Texas Health Science Center, San Antonio, TX 78229, USA

Abstract

Previously, modified release itraconazole in the form of a melt-extruded amorphous solid dispersion based on a pH dependent enteric polymer combined with hydrophilic additives (HME-ITZ), exhibited improved *in vitro* dissolution properties. These properties agreed with pharmacokinetic results in rats showing high and sustained itraconazole (ITZ) systemic levels. The objective of the present study was to better understand the best choice of rodent model for evaluating the pharmacokinetic and efficacy of this orally administered modified release ITZ dosage form against invasive *Aspergillus fumigatus*. A mouse and guinea pig model were investigated and compared to results previously published. In the mouse model, despite similar levels as previously reported values, plasma and lung levels were variable and fungal burden was not statistically different for placebo controls, HME-ITZ and Sporanox ® (ITZ oral solution). This study demonstrated that the mouse model is a poor choice for studying modified release ITZ dosage forms based on pH dependent enteric polymers due to low fluid volume available for dissolution and low intestinal pH. To the contrary, guinea pig was a suitable model to evaluate modified release ITZ dosage forms. Indeed, a significant decrease in lung fungal burden as a result of high and sustained ITZ tissue levels was measured. Sufficiently high intestinal pH and fluids available for dissolution likely facilitated the dissolution process. Despite high ITZ tissue level, the primary therapeutic agent voriconazole exhibited an even more pronounced decrease in fungal burden due to its reported higher clinical efficacy specifically against *Aspergillus fumigatus*.

Keywords

in-vivo absorption; enteric polymers; amorphous solid dispersion; modified release; itraconazole; animal model selection

*Corresponding Author: Department of Pharmaceutics, College of Pharmacy, the University of Texas at Austin, 2409 University Avenue, A1920, Austin, TX 78712, Phone: (512) 471-4681, Fax: (512) 471-7474, bill.williams@austin.utexas.edu.

Declaration of interest

The authors report no conflicts of interest.

Introduction

Invasive fungal infections have emerged as a major cause of morbidity and mortality in immunosuppressed patients [1, 2, 3, 4]. This has been attributed to the increased number of patients suffering from inherited immunodeficiency, cancer, HIV, neutropenia or receiving heart or lung transplantation. *Aspergillus* spp., specifically *Aspergillus fumigatus*, are responsible for the majority of infections caused by filamentous fungi and subsequently are becoming an important public health concern [5]. *Aspergillus fumigatus* infection occurs via spore inhalation and colonization of lung parenchyme. In some cases dissemination to other organs is detected. For instance, dissemination to the brain has been reported and usually leads to poor treatment efficacy [3, 6].

ITZ (structure shown in Figure 1) is a broad-spectrum antifungal drug indicated for the treatment of immunocompromised and non-immunocompromised patients suffering from blastomycosis, coccidioidomycosis, histoplasmosis and aspergillosis [7]. Itraconazole (ITZ) is commercially available in the form of capsules, oral solution (Sporanox ®, Janssen Pharmaceuticals) and tablets manufactured by hot-melt-extrusion processing (Onmel ®, Merz Pharmaceuticals). Due to its low and erratic oral bioavailability [8, 9], a solution containing ITZ and the complexing agent hydroxypropyl-beta-cyclodextrin was introduced, and it reportedly has better absorption than the capsules [10]. Although ITZ itself has an excellent safety profile [7], this cyclodextrin based ITZ oral solution is associated with gastro-intestinal side effects [11, 12]. Furthermore, due to food effect on ITZ absorption, the oral solution has to be taken on an empty stomach [13]. Consequently, an improved ITZ dosage form is of great interest. ITZ is a weakly basic (pKa = 3.7), BCS class II drug exhibiting low and pH dependent solubility (i.e., 5 μg/ml at pH 1 and 1–4 ng/mL at neutral pH) [14] and high lipophilicity (log P = 6.2)[15].

Amorphous solid dispersions, defined as a dispersion of an amorphous drug into a carrier polymer [16], have been gaining increased interest to improve solubility of poorly water soluble drugs, like ITZ. Generally, an amorphous drug has higher free energy and therefore provides an increase in dissolution rate, extent of supersaturation, which usually enables higher bioavailability [17, 18, 19].

Improved solubility and bioavailability of amorphous ITZ in a solid dispersion using enteric polymers (i.e. polymers dissolving at intestinal pH) as a carrier has been reported [18, 21, 22, 23]. DiNunzio et al. showed that amorphous compositions of ITZ and cellulose acetate phthalate produced by Thin Film Freezing results in higher bioavailability in rats due to enhanced intestinal targeting and increased extent and duration of supersaturation [19].

Miller et al. reports that the primary site of ITZ absorption from the rat's gastro-intestinal tract is the proximal small intestine [22]. Based on its pKa and the Henderson-Hasselbach equation, ITZ approaches 99% ionized at pH 1.2, 0.5% ionized at pH 5.5 (dissolution threshold of HPMCAS-LG) and 0% unionized at pH 6.8. It is commonly accepted that unionized drug has higher absorption but lower solubility. Thus, solid dispersion formulations of ITZ and enteric polymers, with the ability to maintain supersaturation in an approximately neutral pH environment, are of interest. Using the pH dependent enteric

acrylic polymer, Eudragit L100-55, solid dispersions with high bioavailability in rats were reported [17]. Furthermore, the addition of Carbopol 934 contributed to stabilizing the degree of ITZ supersaturation, which resulted in further improved absorption [18].

More recently, we reported improved dissolution properties resulting from the addition of hydrophilic additives to enteric ITZ melt-extruded formulations [24]. In particular, low levels (10%) of Vitamin E TPGS (D-α-Tocopheryl polyethylene glycol 1000 succinate), a non-ionic surfactant incorporated into hydroxypropylmethyl-cellulose-acetate-succinate-LG (HPMCAS-LG) based solid dispersion enables controlled drug release in an acidic environment. Upon transition to a neutral environment the HPMCAS-LG matrix can disperse into a colloidal solution and eventually dissolve to supersaturate ITZ [20].

Moreover the presence of low levels of Vitamin E TPGS enhanced drug supersaturation in neutral pH media and prolonged the period of drug supersaturation (which was not due to the solubilization by the surfactant). These dissolution properties, improved over that of commercial itraconazole capsules, were in agreement with the pharmacokinetic results in rats in which high and sustained ITZ systemic levels were reported [24]. Vitamin E TPGS, mainly used as an absorption and bioavailability enhancer [26], has also been reported to inhibit CYP3A4 [26], the enzyme responsible for metabolizing ITZ [27, 28]. Therefore, besides the improved dissolution properties, the presence of Vitamin E TPGS in the formulation inhibited the enzymatic activity of CYP 3A4 leading to decreased ITZ metabolism and subsequent higher blood levels of drug [24].

In the present study, following these encouraging pharmacokinetic results in rats [24], we sought to demonstrate efficacy against fungal infection of this modified release ITZ dosage (HME-ITZ). Due to unavailability of rats as an *Aspergillus fumigatus* disease model in our facility, mice and guinea pigs were selected as animal models to evaluate efficacy of the dosage form. VCZ, which is the primary therapy for invasive pulmonary aspergillosis [40], was used as a positive control in the guinea pig model. In mice, due to extensive metabolism and high clearance of VCZ, posaconazole was used as the positive control. Differences between the guinea pig and mouse models were determined by a dose tolerability study that included an assessment of pharmacokinetic profiles of the formulation at different dosing regimens and an efficacy study using immunocompromised animals infected with *Aspergillus fumigatus*.

Materials

ITZ was purchased from Letco (Decatur, AL). HPMCAS-LG was kindly donated by Shin-Etsu (Totowa, NJ). Vitamin E TPGS was purchased from Antares Health Products, Inc. (St. Charles, IL) and Triethylcitrate was kindly donated by Vertellus Performance Materials, Inc (Greensboro, NC).

Sodium phosphate tribasic, sodium phosphate monobasic monohydrate, sodium hydroxide, diethylamine (DEA) were purchased from Fischer Scientific (Waltham, MA). High-performance liquid chromatography (HPLC) solvents were HPLC grade. All other chemicals utilized in this study were ACS grade.

Methods

Hot-Melt Extrusion and Size Reduction of Extrudate

The melt extruded formulation (HME-ITZ) was manufactured with a HAAKE Minilab II micro Compounder (Thermo Electron Corporation, Newington, NH) equipped with twin, co-rotating conical screws (5/14 mm diameter). 29.4% ITZ, 58.8% HPMCAS-LG plasticized with 5.9% Vitamin-E TPGS and 5.9% Triethyl Citrate were mixed before extrusion. The powder blends were fed manually into the extruder barrel. The hot-melt extruder was run without a die. The cross section of the melt extrudate was shaped into a 1.0×4.0 mm rectangle. The processing temperature and screw rotating speed were set to 160°C and 150 rpm, respectively. After extrusion, the extrudates were cooled to room temperature and milled with a Fitzmill (Model L1A Comminuting Machine, The Fitzpatrick Company, Elmhurst, IL) using knife mode blades and a rotating speed of 9,000 rpm. The screen size for the milling chamber screen was 0.020 inches.

Powder extrudate recovered following milling of the extrudate were cryo-milled using a Spex SamplePrep 6870 Freezer/Mill (Metuchen, NJ, USA). Samples were placed in polycarbonate vials with a magnetically driven impactor. Samples were immersed in liquid nitrogen, pre-cooled for 10 min, milled for 2 min. at a frequency of 10 cycles per second (cps), followed by a pause of 2 min. This cycle was repeated three times.

Particle size fractions analysis

Particle size was measured using sonic sieving (Sonic Sifter Separator, Advantech Manufacturing New Berlin, WI) during 10 minutes. The sonic sifter was equipped with sieves of the following opening sizes: 125 μm, 90 μm, 63 μm, 45 μm, < 45 μm. Particles below 125 μm were used for this study.

Dissolution Testing in pH Transition Conditions

Dissolution studies were conducted according to USP 29 apparatus II (paddle). A VanKel VK 7000 dissolution system (Varian, Inc., Palo Alto, CA) was used to perform the testing. The paddle speed and temperature were set to 75 rpm and 37±0.5°C, respectively. 750 mL of 0.1N HCl (pH 1.2) aqueous solution was added in the dissolution vessel to pre-heat the media before testing. An extrudate aliquot containing 37.5 mg ITZ equivalent was added in the dissolution vessel. At the 2-hour time point, 250 mL of pre-heated (37°C) basic solution (0.2M Na3PO4) were added into the dissolution media, and the pH of the media was adjusted to 6.8. Aliquots were taken at the following time points: 30 min, 1 hr, 2 hr, 2 hr 10 min, 2 hr 20 min, 2.5 hr, 3 hr, 4 hr, 6 hr, and 8 hr. Each aliquot was filtered through a 0.2 μm, 13 mm PTFE membrane filter (Wheaton, Millville, NJ) and analyzed by HPLC.

High Pressure Liquid Chromatography (HPLC)

Drug levels were measured using a Dionex HPLC system (Thermo Fisher Scientific Inc., Waltham, MA). Specifically, for *in vitro* measurements, ITZ was detected using an Inertsil® ODS-2 column (5 μm, 4.6×150 mm). The composition of HPLC mobile phase was acetonitrile:water:DEA (700:300:0.5). Mobile phase was filtered through a 0.2 μm PTFE filter, degassed under vacuum and sonicated prior to use. The mobile phase flow rate was 1

mL/min. The column temperature was maintained at 25°C. The retention time of ITZ was about 5.5 min. The detection wavelength was set to 263 nm.

For *in vivo* measurements, ITZ and hydroxy-Itraconazole (OH-ITZ) were detected using a Phenomenex CAPCELL C18 UG 120 HPLC column (5 μm, 4.6 mm×250 mm). A volume of 620 mL of acetonitrile was mixed with 380 mL phosphate buffer solution at pH 6.7. Mobile phase was filtrated through a 0.2 μm PTFE filter to remove any particles and degassed under vacuum and sonication prior to use. The mobile phase flow rate was 1 mL/min. The column temperature was maintained at 37°C. The detection wavelength was set to 263 nm.

In Vivo Study

Animal experiments were conducted in full compliance with UT Health Science Center guidelines in agreement with the Association for Assessment and Accreditation of Laboratory Animal Care (AAALAC), the Animal Welfare Act (AWA) and the Guide for the Care and Use of Laboratory Animals. This institutionally approved study was conducted at UTHSCSA with male ICR mice and guinea pigs in established models of invasive pulmonary aspergillosis [41, 42, 43, 44, 45].

Male Guinea pigs and male ICR mice had average body weight of 500 g and 25 g, and were between 5 to 7 weeks and 3 to 4 weeks old, respectively. A standard neutropenic immunosuppression regimen was used in each model. Bacterial superinfection and deaths in the immunosuppressed animals were prevented by antibiotic propyhylaxis with enrofloxacin administration subcutaneously beginning the day after animals arrived and continuing daily until the end of the experiment.

Throughout the course of experiments, animals were monitored at least twice daily to prevent and minimize unnecessary pain and distress. Moribund animals were humanely euthanized. During the length of the study, animals had access to food and water *ad libitum*.

Dose tolerability experiments were conducted in immunosuppressed and uninfected animals. Mice were given four oral HME-ITZ doses: 10 mg/kg three times per day (TID), 15 mg/kg two times a day (BID), 20 mg/kg TID and 30 mg/kg BID. HME-ITZ was suspended in a 2% hydroxypropyl cellulose solution at the desired concentration such that mice were administered 0.2 mL by oral gavage while guinea pigs were administered 2.5 mL. Guinea pigs were investigated only for two different doses of 15 and 30 mg/kg BID for 7 days. Following the morning dose on day 7, blood was collected from anesthetized animals at various time points (i.e., 1, 2, 4, 8, 12, and 24 hours), and the plasma was separated. In mice, 0.5 to 1 mL plasma was collected in isoflurane anesthetized animals by exsanguination via cardiac puncture (as a terminal procedure). In guinea pig, ketamine and xylazine were administered intramuscularly then 1 to 2 mL was collected from the saphenous vein. Lungs were also collected following the terminal blood collection (i.e., at time points 8, 12, and 24 hours) for measurement of ITZ concentrations.

After collection, plasma (200 μL) was transferred to a clean 1.5 mL tube. In order to precipitate plasma proteins, 50 μL of 0.3N barium hydroxide and 50 μL of 0.4N zinc sulfate heptahydrate were added. The mixture was vortex mixed 30 s. Then 1 mL of internal control

ketoconazole solution (0.5 μg/mL in acetonitrile) was added into the tube and mixed for another 1.5 min. The mixture was centrifuged at 8000 rpm for 10 min. The supernatant was transferred to another 1.5 mL tube. The tube was placed in a metal heating block (70°C) under a stream of nitrogen. The sample was re-constituted using 250 μL of mobile phase and mixed for 1 min, followed by a centrifugation at 8000 rpm for 10 min. A 200 μL of the supernatant was transferred into a 300 μL HPLC vial.

Following euthanasia, the chest cavity was opened under aseptic conditions and the lungs were removed and weighed. Lungs were cut into approximately 0.4 g portions and added to a 1.5 mL tube with 1 mL saline, homogenized by sonication for 1 min. 200 μL were transferred into 1.5 mL tube and ITZ was extracted following the same procedure as plasma samples. All samples were analyzed via HPLC following the method outlined above.

The efficacy study was conducted in infected animals. *Aspergillus fumigatus* clinical isolate 293 was the organism utilized to establish infection. To simulate the pathogenesis of invasive aspergillosis, animals were inoculated using an established whole body aerosol chamber within a Class II A2 biosafety cabinet for a one-hour duration exposure to *Aspergillus fumigatus* conidia, as published previously [41, 42, 43]. Treatment with antifungals began 24 hours following inoculation and continued through day 7 post-inoculation. Two dosing regimens selected during the dose tolerability study were investigated for each animal model. HME-ITZ suspended in HPC 2% aqueous solution and the positive control, VCZ for guinea pig and posaconazole for mice, were administered by oral gavage.

Tissue fungal burden were measured using enumeration of colony-forming units (CFU) in lungs after 48 – 72 hours (until growth of individual colonies large enough to count but not long enough for them to grow together). One gram of lung tissue from each animal was weighed and homogenized in sterile saline. Serial dilutions of the homogenate were prepared and plated onto potato dextrose agar. After a period of incubation, the number of *A. fumigatus* colonies were counted and CFU/gram of lung tissue determined. If necessary, a more accurate measurement by real-time PCR was also used to measure pulmonary fungal burden. The amount of DNA per sample was measured by qPCR with the use of an ABI PRISM 7300 sequence detection system (Applied Biosystems) with primers and a dual-labeled fluorescent hybridization probe specific for the *A. fumigatus* (1→3)-β-D-glucan synthase gene (AFKS; GeneBank accession number U79728).

Blood and lungs were collected on day 8 from anesthetized animals via cardiac puncture as a terminal procedure. The primary outcome criteria were changes in pulmonary fungal burden as measured by CFU and, if necessary, quantified more accurately by qPCR. Differences in pulmonary fungal burden were assessed for significance in both animal models by analysis of variance with Tukey's post-test for multiple comparisons of parametric data, and the Kruskal-Wallis test with Dunn's post-test for multiple comparisons was used for nonparametric data. A p-value of < 0.05 was considered statistically significant for all comparisons. ITZ and OH-ITZ concentration in plasma and lung tissues on day 8 were also evaluated. In the guinea pig model, after observation of a moribund animal, it was hypothesized that drug could have permeated to the brain, thus drug concentration was measured on day 8 in the brain of each guinea pig.

The treatment's overall efficacy in mice was evaluated in parallel by a survival study in which mice were followed through day 12 for survival, 5 days after treatment stopped. Survival was plotted by Kaplan-Meier analysis, and differences in median survival time, and the percent survival among groups was analyzed by the log-rank test and Fischer's exact test, respectively.

Results

Formulation Characterization

HME-ITZ samples exhibited a single glass transition temperature at about 45°C and no crystalline peak confirming the formation of a single-phase amorphous dispersion (data not shown) by mDSC. For more information on HME-ITZ formulation development and characterization the reader is referred to Lang et al [24]. The results of HME-ITZ dissolution in pH transition conditions before and after cryo-milling are shown in Figure 2, while values of area under dissolution curves (AUDC) are shown in Table 1. Cryo-milled HME-ITZ exhibited a higher dissolution extent in acidic media and subsequently a considerably greater $AUDC_{acid}$ (more than 5-times that of non cryo-milled HME-ITZ). This can be related to the particle size, which showed smaller particle size after cryo-milling. Particle size fraction below 45 μm (21.1% cryo-milled vs. 5.6% for non cryo-milled particles) and between 45 μm and 90 μm (57.4% vs. 21.1%) were increased thanks to cryo-milling, while the fraction between 90 and 125 μm (21.5% vs. 73.3%) was decreased. In neutral media, $AUDC_{neutral}$ was similar for both particle sizes confirming that the cryo-milling step did not affect the polymeric enteric properties or extent of supersaturation.

Pharmacokinetic and pharmacodynamic study in mice

For mice, plots of concentration vs. time in plasma and in lungs for ITZ and its active metabolite OH-ITZ are shown in Figures 3 and 4. Based on these results and those presented in Table 2, the highest ITZ and OH-ITZ [46, 47] levels in serum were attained following 30 mg/kg BID dosing (C_{max} at 2.06 μg/mL and 0.93 μg/mL, respectively). However, in lungs, a lower dose, 15 mg/kg BID led to the highest ITZ and OH-ITZ levels (AUC_{t0-8h} of 22.36 μg.h / mL and a C_{max} of 4.98 μg/g and 3.02 μg/g for ITZ and OH-ITZ, respectively). Despite the linear pharmacokinetic data previously reported for ITZ, no correlation was found between the dose and tissue concentrations in mice (n= 3 mice per time point).

Similarly, the lowest levels in plasma and lungs were achieved following dosing with two different dosing regimens. A dose of 10 mg/kg TID led to the lowest ITZ and OH-ITZ levels in plasma. More surprisingly, at 20 mg/kg TID dosing, despite its high dose per day, led to the lowest lung levels.

Fungal burden was evaluated in mice as an indication of antifungal efficacy; results are presented in Figure 5. None of the HME-ITZ dosing regimen resulted in a statistically different decrease in fungal burden in mice. The ITZ oral solution Sporanox® did not decrease fungal burden, either. To the contrary, the positive control posaconazole significantly decreased fungal burden from 4.19 ± 0.4 CFU/g in the control group to 1.81 ±1.0 CFU/g ($p<0.0001$).

The outcomes of the survival study are presented in Figure 6. The HME-ITZ and Sporanox® dosed animals died or were euthanized before day 7 (median survival of 5, 7 and 6.5 days for HME ITZ 15 mg/kg BID, HME-ITZ 30 mg/kg BID and Sporanox 15 mg/kg, respectively). Owing to a decreased fungal burden in mice treated with posaconazole, 70% survival (p=0.0010) was observed in this group on day 12, the survival arm endpoint.

Following the pharmacodynamic study on day 8, 24 hours after the end of treatment, ITZ and OH-ITZ levels were below quantification limits in mice plasma and lungs. The limit of detection and quantification reported for this method are 10 ng/mL and 30 ng/mL, respectively [48].

Pharmacokinetic and pharmacodynamic study in guinea pig

In the guinea pig model, concentration vs. time profiles for ITZ and OH-ITZ in lungs and plasma, shown in Figures 7 and 8, were quite different from the results found in the mouse model. Plasma and lung C_{max} were as high as 2.54 μg/mL and 42.02 μg/g, respectively, for the 30mg/kg BID dose; whereas the 15 mg/kg BID dose had an ITZ C_{max} of 1.38 μg/mL and 19.35 μg/g in plasma and lung, respectively. These results indicate a relationship between doses administered and C_{max}. This relationship was also found for the $AUC_{t0\text{-}8h}$ with levels at 5.92 μg. h/mL and 12.94 μg. h/mL in plasma, and 77.68 μg. h/mL and 148.84 μg. h/mL in lungs. Doubling of the administered dose led to about a 2-fold increase in ITZ C_{max} and $AUC_{t0\text{-}8h}$.

OH-ITZ concentrations were less than ITZ levels, but generally exhibited the same plasma concentration profile; C_{max} of approximately 0.73 μg/mL and 4.38 μg/g in plasma and lungs, respectively, for the 30 mg/kg BID dose were found.

ITZ and OH-ITZ concentration profiles were similar in plasma as well as in lungs. However, even though the T_{max} of the two dosing regimens was similar in plasma, in lungs, dosed at 15 mg/kg BID, had a shorter T_{max} (T_{max} = 2h) than 30 mg/kg BID (T_{max} = 5h). This was found for both ITZ and OH-ITZ.

In the guinea pig model, as shown in Figure 9, HME-ITZ 30 mg/kg BID dosing led to a significant decrease in fungal burden while 15 mg/kg dosing regimen was not statistically different from placebo. A more precise quantification of the fungal burden was conducted via qPCR measurement, which showed significantly decreased fungal burden for HME-ITZ 15 mg/kg BID and 30 mg/kg BID, respectively 21.6 ng/mL (p=0.0094) and 15.5 ng/mL (p=0.0086). In comparison, a mean of 652 ng/mL was measured for guinea pigs receiving the placebo (i.e., the suspension vehicle, 2% HPC solution). These results demonstrated the efficacy of this formulation against *Aspergillus fumigatus*. However VCZ positive controls exhibited an even more pronounced and significant efficacy with fungal DNA levels as low as 0.54 ng/mL (p=0.0069). As expected, no fungal burden was present in uninfected controls.

Following the pharmacodynamic study on day 8, guinea pig plasma and brain samples were collected to measure drug concentration (Table 3). In plasma, high ITZ levels for the two dosing regimens investigated were found 24 hours after the last dose (1.04 μg/mL for 15

mg/kg BID and 2.49 μg/mL for 30 mg/kg BID). In brain, ITZ levels were surprisingly high; levels up to 9.39 μg/g were measured (30 mg/kg BID dosing regimen). To the contrary, OH-ITZ brain levels were relatively low as compared to plasma levels.

Discussion

Cryo-milled HME-ITZ showed an increased dissolution in acidic media without affecting the degree of supersaturation obtained in neutral pH media. The increased dissolution rate in acidic media was likely due to the smaller particle size of the cryo-milled extrudates. In fact, this can be explained by the Nernst-Brunner equation, which demonstrates the impact of surface area, and therefore particle size on dissolution rate [49].

Interestingly, higher supersaturation levels in acidic media did not lead to faster precipitation in neutral pH, contrary to higher supersaturation obtained by increasing the amount of vitamin E TPGS [24]. This result demonstrated that supersaturation and re-crystallization in neutral media were driven by the formulation and essentially by the stabilization and re-crystallization inhibition effect provided by HPMCAS-LG [20].

In vivo relationship between the dose administered and the ITZ pharmacokinetic parameters has previously been reported in rats and mice [50, 51, 52]. Indeed, an increased ITZ dose led to an increase in $AUC_{t0\text{-}8h}$ and C_{max}. In some studies, it has been reported that the increase in pharmacokinetic parameters is even greater than the proportional dose increase. In the present study in mice, the absence of relationship between dose and pharmacokinetic parameters is likely explained by the inability of mice GI tract to dissolve or disperse entirely the enteric polymer particles. Indeed, as previously described by McConnell et al [31] the gastro-intestinal tract pH values in mice are different from those in man and other commonly used animal models such as rats, guinea pigs or beagle dogs. Table 4 compares the characteristics of the GI tract in mice, rats and guinea pigs. In mice, relatively high stomach pH (pH 4 in fasted state) and low intestinal pH (pH 5 or 4.8 in the fasted and fed state, respectively) are reported. These values, below the pH dissolution/dispersion threshold of the pH dependent polymer, HPMCAS-LG, likely hindered the complete dispersion of the polymer and therefore prevented complete release of ITZ. Besides the differences in pH, the low volume of fluid available in the GI tract of mice is also a concern and may have impacted polymer and drug dissolution; fluid volumes of 0.6 to 0.8 g have been reported in the mouse intestine [31]. For comparison rats have fluid volumes of 3.0–4.6 g and intestinal pH up to 7.5, which could explain, in theory, the satisfactory results obtained previously in rats. Additionally, the reported length of mice intestine is approximately two times shorter than in rats, decreasing thereby the absorption window.

To our knowledge, *in vivo* assessment of modified release ITZ amorphous solid dispersions based on a pH dependent enteric polymer has not been reported in mice. Based on our pharmacokinetic results and the values reported in the literature for mice, we conclude that the GI tract of mice is not suitable to evaluate these types of formulations that contain a pH dependent polymer, in which high pH and sufficient fluid volumes are necessary to disperse and dissolve the polymer and drug.

A study conducted by our group, following the same protocol as the present study, allowed comparison with our results. C_{max} of 0.99 μg/mL and 1.5 μg/g were reported in lungs following 30 mg/kg TID Sporanox® solution administered over 8 days to ICR mice [54]. Both plasma and lung levels with HME-ITZ administration were higher for each dosing regimen (except for the 20 mg/kg dose administered TID) compared to Sporanox ® solution. This demonstrated improved pharmacokinetic parameters of the HME-ITZ formulation even at lower administered doses compared to Sporanox ® solution, despite the impediment of complete polymer dispersion in mice GI tract This can be explained by the increased solubility of amorphous ITZ but also by the lower permeability obtained with formulations containing cyclodextrin (e.g. Sporanox ® solution), compared to amorphous solid dispersions [55]. This phenomenon is explained by a decreased apparent permeability due to the increased apparent solubility.

In another recent study in ICR mice, oral ITZ was compared to pulmonary administration of ITZ by nebulization [48]. Plasma and lung levels were assessed following 8 days of treatment and 12 hours after the last dose. HME-ITZ had better pharmacokinetic results than pulmonary administration of ITZ (at this specific time point). Indeed, after 12 hours, ITZ trough level was slightly higher for HME-ITZ in plasma (0.5 μg/mL compared to 0.35 μg/mL) and in lungs (2.5 μg/mL compared to 2.25 μg/mL). Even though these differences cannot be considered significant, they demonstrate that HME-ITZ enables, at least, similar levels as a pulmonary administration of ITZ: that being moderate plasma levels (enabling decreased side effects) and high lung levels (permitting high efficacy against fungal infections in the lungs). Plasma levels for ITZ and OH-ITZ were higher than previously reported results in rats. However, because the protocol and dosing regimen were different (single dose in rats), the two animal species could not be directly compared.

Even though a dose/concentration relationship was not found in the present mouse study, plasma and lung levels were sufficiently high to expect a clinical effect. However, despite these high levels exhibited by HME-ITZ, no clinical efficacy was observed, which highlighted another issue encountered with ITZ studies in mice. Indeed, besides the variability in pharmacokinetics, mice present a paradox due to low success of ITZ therapy in spite of high tissue levels [33, 34]. Papers previously published on ITZ efficacy in mice following oral dosing demonstrated that high doses were usually necessary to observe an improvement in efficacy against invasive fungal infections. These doses were dependent on the mouse model used for each study. Van't Wout et al. needed 40 mg/kg doses in order to observe a modest antifungal effect in Swiss mice [34]. This dose being higher than the one used in previous studies was explained by differences in cellular host defense animals and the time elapsed between infection and treatment. Similarly, 80% of ICR mice treated with ITZ 100 mg/kg/day died by day 30 [33]. Doses higher than 320 mg/kg (single dose) were reported necessary to have a 50% effect in mice species [56]. It is important to note here that the outcome of therapy is not only dependent on intensive antifungal therapy, but also on recovering host defense defects, which can explain the efficacy differences between different species [3].

On the other hand, efficacy experiments in guinea pigs led to clinical improvements at a lower dose and tissue concentrations [35, 36]. This paradox and low efficacy of ITZ against fungal infections in mice remains unexplained but corroborates our results.

In guinea pigs, the pharmacokinetic profile of ITZ following oral administration is also different from mice. Using this model, our results demonstrated the pharmacokinetic relationship between the two ITZ doses investigated, the $AUC_{t0\text{-}8h}$ and the C_{max}. A two-fold increase in the administered dose led to a two-fold increase in the $AUC_{t0\text{-}8h}$ and C_{max}. These results are in agreement with the relationship previously discussed between ITZ dose and pharmacokinetic parameters *in vivo*. Previous reports testing ITZ in guinea pigs led to lower C_{max} compared to the results reported in this present study. For instance, a single oral dose at 20 mg/kg of ITZ gave C_{max} values of 0.70 μg/mL [57] and C_{max} of 1.17 μg/mL (after a 20 mg/kg dose) was reported following ITZ-cyclodextrin complex administration [39]. Even though these levels are lower than the one we report for HME-ITZ (1.38 μg/mL and 2.54 μg/mL for 15 mg/kg and 30 mg/kg), no conclusion can be drawn due to the difference in dosing regimen. Importantly, it has also been demonstrated that grapefruit juice increased ITZ levels following oral dosing only in the guinea pig model, thereby confirming the effect of grapefruit juice in the GI tract as described for humans [39]. Therefore, we hypothesize that upon its release from the pH dependent enteric polymer, Vitamin E TPGS, which is a reported CYP3A4 inhibitor, eventually contributed to decreasing the rate of metabolism of ITZ.

The relationship between dose and pharmacokinetic results reported with HME-ITZ formulation in guinea pigs suggested that potentially, the drug was completely dissolved and absorbed. This agrees with the guinea pig GI tract description detailed by Merchant et al. [32] and included in Table 4. Indeed, upon transition from the stomach to the intestine, the pH increases from 2.9 to ~ 6 – 7.4 in the fed state. These pH values in the intestine are sufficiently high to dissolve and/or disperse the enteric polymer and the high volumes of fluid available (~ 38 g) also aid the dissolution process. The authors reported that pH changes along the GI tract are closer to man. Due to higher pH values, larger fluid volume, and longer length of the small intestine, it appears that the guinea pig is a more suitable model than mice to evaluate enteric polymer-based formulations.

The guinea pig model exhibited high and sustained ITZ and OH-ITZ levels in plasma and lungs. The high pH in guinea pig intestine and the large volumes available enable the dissolution and dispersion of the polymer matrix into a colloidal solution permitting drug release [20]. Furthermore, as explained previously the amorphous state of the drug and the presence of HPMCAS-LG enables supersaturated concentration *in vivo* in guinea pig intestine and enhanced absorption. The presence of vitamin E TPGS likely contributed to enhanced permeation of ITZ. The high extent of drug release and its permeation to the lungs enable a significant decrease in the fungal burden as demonstrated with the fungal DNA qPCR levels. However, the differences between the two doses are not statistically significant.

All guinea pigs treated with HME-ITZ survived after 8 days whereas in the VCZ treatment group, one animal died at the end of the study. Nevertheless, 10 mg/kg VCZ positive control was significantly more effective at decreasing the fungal burden than HME-ITZ

formulations. This is likely explained by the higher efficacy of VCZ specifically against *Aspergillus fumigatus* [58]. Indeed, VCZ is the reference treatment against *Aspergillus fumigatus* [40], and this justifies the selection of VCZ as the reference treatment allowing the HME-ITZ formulation to be challenged.

Interestingly, at the end of the pharmacodynamic study, 24 hours after the last dose, we found high plasma ITZ levels that were likely due to the extent of supersaturation provided by HPMCAS-LG and Vitamin E TPGS, and also probably to the inhibiting action of the latter on ITZ CYP3A4 metabolism and P-glycoprotein [59].

After observation of one moribund guinea pig, the brain of all guinea pigs were collected for ITZ assay. Central nervous systems (CNS) infections by *Aspergillus fumigatus* have been reported in humans. These CNS infections usually result in poor clinical outcomes even with therapy, as only 6% of patients having disseminated *Aspergillus fumigatus* to the CNS had complete responses when treated [3]. This was significantly lower than dissemination to other organs. The low penetration of ITZ into the CSF may partly explain this lack of efficacy [6]. However, in the present study, high levels of ITZ were measured in the brain, which would likely help decrease fungal infections if dissemination to the CNS occurred. High and sustained levels of ITZ provided by the HME-ITZ formulation and the benefit of vitamin E TPGS as an absorption enhancer and CYP450 inhibitor can also explain these high levels found in guinea pig brain.

Conclusion

To our knowledge this is the first study reported for modified release dosage forms based on a pH dependent enteric polymer in mice. Due to high variability in ITZ efficacy, low intestinal pH and fluid volumes, the mouse model was not a suitable model to evaluate a dosage form containing HPMCAS-LG. To the contrary, guinea pigs, which present GI properties closer to that of humans, allowed a better dissolution and dispersion of the enteric matrix as demonstrated by high and sustained ITZ levels and the relationship between the two HME-ITZ dose and ITZ pharmacokinetic parameters (C_{max} and $AUC_{t0\text{-}8h}$). Clinically, in guinea pigs, these high levels permitted a decrease in *Aspergillus fumigatus* fungal burden, which allowed their survival. Therefore, guinea pigs appeared as a more suitable model to assess performance of ITZ enteric-based solid dispersion formulations in comparison to mice.

Acknowledgments

This project utilized preclinical services funded by the National Institute of Allergy and Infectious Diseases, National Institutes of Health, Department of Health and Human Services, under Contract No.HHSN272201000038I - Task Order A05.

References

1. Denning DW. Invasive aspergillosis. Clinical infectious diseases : an official publication of the Infectious Diseases Society of America. 1998; 26:781–803. [PubMed: 9564455]
2. Taccone FS, Van den Abeele AM, Bulpa P, Misset B, Meersseman W, Cardoso T, Paiva JA, Blasco-Navalpotro M, De Laere E, Dimopoulos G, Rello J, Vogelaers D, Blot SI. Asp ICUSI.

Epidemiology of invasive aspergillosis in critically ill patients: clinical presentation, underlying conditions, and outcomes. Crit Care. 2015; 19:7. [PubMed: 25928694]

3. Patterson TF, Kirkpatrick WR, White M, Hiemenz JW, Wingard JR, Dupont B, Rinaldi MG, Stevens DA, Graybill JR. Invasive aspergillosis. Disease spectrum, treatment practices, and outcomes. I3 Aspergillus Study Group. Medicine. 2000; 79:250–60. [PubMed: 10941354]
4. Meersseman W, Van Wijngaerden E. Invasive aspergillosis in the ICU: an emerging disease. Intensive Care Med. 2007; 33:1679–81. [PubMed: 17646965]
5. Dagenais TR, Keller NP. Pathogenesis of Aspergillus fumigatus in Invasive Aspergillosis. Clin Microbiol Rev. 2009; 22:447–65. [PubMed: 19597008]
6. Lutsar I, Roffey S, Troke P. Voriconazole concentrations in the cerebrospinal fluid and brain tissue of guinea pigs and immunocompromised patients. Clinical infectious diseases : an official publication of the Infectious Diseases Society of America. 2003; 37:728–32. [PubMed: 12942409]
7. Odds FC. Itraconazole - a new oral antifungal agent with a very broad spectrum of activity in superficial and systemic mycoses. Journal of Dermatological Science. 1993; 5:65–72. [PubMed: 8395201]
8. Denning DW, Tucker RM, Hanson LH, Stevens DA. Treatment of invasive aspergillosis with itraconazole. Am J Med. 1989; 86:791–800. [PubMed: 2543220]
9. Smith D, van de Velde V, Woestenborghs R, Gazzard BG. The pharmacokinetics of oral itraconazole in AIDS patients. The Journal of pharmacy and pharmacology. 1992; 44:618–9. [PubMed: 1357148]
10. Barone JA, Moskovitz BL, Guarnieri J, Hassell AE, Colaizzi JL, Bierman RH, Jessen L. Enhanced bioavailability of itraconazole in hydroxypropyl-beta-cyclodextrin solution versus capsules in healthy volunteers. Antimicrobial agents and chemotherapy. 1998; 42:1862–5. [PubMed: 9661037]
11. Vandewoude K, Vogelaers D, Decruyenaere J, Jaqmin P, De Beule K, Van Peer A, Woestenborghs R, Groen K, Colardyn F. Concentrations in Plasma and Safety of 7 Days of Intravenous Itraconazole Followed by 2 Weeks of Oral Itraconazole Solution in Patients in Intensive Care Units. Antimicrobial agents and chemotherapy. 1997; 41:2714–8. [PubMed: 9420044]
12. Winston DJ, Maziarz RT, Chandrasekar PH, Lazarus HM, Goldman M, Blumer JL, Leitz GJ, Territo MC. Intravenous and oral itraconazole versus intravenous and oral fluconazole for long-term antifungal prophylaxis in allogeneic hematopoietic stem-cell transplant recipients. A multicenter, randomized trial. Ann Intern Med. 2003; 138:705–13. [PubMed: 12729424]
13. Janssen Pharmaceutical Inc. [Accessed 25 Apr 2016] Sporanox (Itraconazole capsule) Prescribing information2015Available from: http://www.janssen.com
14. Jung JY, Yoo SD, Lee SH, Kim KH, Yoon DS, Lee KH. Enhanced solubility and dissolution rate of itraconazole by a solid dispersion technique. International journal of pharmaceutics. 1999; 187:209–18. [PubMed: 10502627]
15. Peeters J, Neeskens P, Tollenaere JP, Van Remoortere P, Brewster ME. Characterization of the interaction of 2 - hydroxypropyl - β - cyclodextrin with itraconazole at pH 2, 4, and 7. Journal of pharmaceutical sciences. 2002; 91:1414–22. [PubMed: 12115841]
16. Chiou WL, Riegelman S. Pharmaceutical applications of solid dispersion systems. Journal of pharmaceutical sciences. 1971; 60:1281–302. [PubMed: 4935981]
17. Miller DA, DiNunzio JC, Yang W, McGinity JW, Williams RO III. Enhanced in vivo absorption of itraconazole via stabilization of supersaturation following acidic-to-neutral pH transition. Drug development and industrial pharmacy. 2008; 34:890–902. [PubMed: 18608468]
18. Miller DA, DiNunzio JC, Yang W, McGinity JW, Williams RO III. Targeted intestinal delivery of supersaturated itraconazole for improved oral absorption. Pharmaceutical research. 2008; 25:1450–9. [PubMed: 18288449]
19. DiNunzio JC, Miller DA, Yang W, McGinity JW, Williams RO III. Amorphous compositions using concentration enhancing polymers for improved bioavailability of itraconazole. Molecular pharmaceutics. 2008; 5:968–80. [PubMed: 19434851]
20. Friesen DT, Shanker R, Crew M, Smithey DT, Curatolo WJ, Nightingale JA. Hydroxypropyl methylcellulose acetate succinate-based spray-dried dispersions: an overview. Molecular pharmaceutics. 2008; 5:1003–19. [PubMed: 19040386]

21. Six K, Daems T, de Hoon J, Van Hecken A, Depre M, Bouche MP, Prinsen P, Verreck G, Peeters J, Brewster ME, Van den Mooter G. Clinical study of solid dispersions of itraconazole prepared by hot-stage extrusion. European journal of pharmaceutical sciences : official journal of the European Federation for Pharmaceutical Sciences. 2005; 24:179–86. [PubMed: 15661489]
22. Miller DA, McConville JT, Yang W, Williams RO III, McGinity JW. Hot-melt extrusion for enhanced delivery of drug particles. Journal of pharmaceutical sciences. 2007; 96:361–76. [PubMed: 17075869]
23. Overhoff KA, Moreno A, Miller DA, Johnston KP, Williams RO III. Solid dispersions of itraconazole and enteric polymers made by ultra-rapid freezing. International journal of pharmaceutics. 2007; 336:122–32. [PubMed: 17184938]
24. Lang B, Liu S, McGinity JW, Williams RO III. Effect of hydrophilic additives on the dissolution and pharmacokinetic properties of itraconazole-enteric polymer hot-melt extruded amorphous solid dispersions. Drug development and industrial pharmacy. 2016; 42:429–45. [PubMed: 26355819]
25. Sotthivirat S, McKelvey C, Moser J, Rege B, Xu W, Zhang D. Development of amorphous solid dispersion formulations of a poorly water-soluble drug, MK-0364. International journal of pharmaceutics. 2013; 452:73–81. [PubMed: 23651642]
26. Guo Y, Luo J, Tan S, Otieno BO, Zhang Z. The applications of Vitamin E TPGS in drug delivery. European journal of pharmaceutical sciences : official journal of the European Federation for Pharmaceutical Sciences. 2013; 49:175–86. [PubMed: 23485439]
27. Isoherranen N, Kunze KL, Allen KE, Nelson WL, Thummel KE. Role of itraconazole metabolites in CYP3A4 inhibition. Drug metabolism and disposition: the biological fate of chemicals. 2004; 32:1121–31. [PubMed: 15242978]
28. Peng CC, Shi W, Lutz JD, Kunze KL, Liu JO, Nelson WL, Isoherranen N. Stereospecific metabolism of itraconazole by CYP3A4: dioxolane ring scission of azole antifungals. Drug metabolism and disposition: the biological fate of chemicals. 2012; 40:426–35. [PubMed: 22106171]
29. Andriole VT. The 1998 Garrod lecture. Current and future antifungal therapy: new targets for antifungal agents. The Journal of antimicrobial chemotherapy. 1999; 44:151–62. [PubMed: 10473222]
30. Sjogren E, Abrahamsson B, Augustijns P, Becker D, Bolger MB, Brewster M, Brouwers J, Flanagan T, Harwood M, Heinen C, Holm R, Juretschke HP, Kubbinga M, Lindahl A, Lukacova V, Munster U, Neuhoff S, Nguyen MA, Peer A, Reppas C, Hodjegan AR, Tannergren C, Weitschies W, Wilson C, Zane P, Lennernas H, Langguth P. In vivo methods for drug absorption - comparative physiologies, model selection, correlations with in vitro methods (IVIVC), and applications for formulation/API/excipient characterization including food effects. European journal of pharmaceutical sciences : official journal of the European Federation for Pharmaceutical Sciences. 2014; 57:99–151. [PubMed: 24637348]
31. McConnell EL, Basit AW, Murdan S. Measurements of rat and mouse gastrointestinal pH, fluid and lymphoid tissue, and implications for in-vivo experiments. The Journal of pharmacy and pharmacology. 2008; 60:63–70. [PubMed: 18088506]
32. Merchant HA, McConnell EL, Liu F, Ramaswamy C, Kulkarni RP, Basit AW, Murdan S. Assessment of gastrointestinal pH, fluid and lymphoid tissue in the guinea pig, rabbit and pig, and implications for their use in drug development. European journal of pharmaceutical sciences : official journal of the European Federation for Pharmaceutical Sciences. 2011; 42:3–10. [PubMed: 20932902]
33. Sugar AM, Liu XP. Interactions of itraconazole with amphotericin B in the treatment of murine invasive candidiasis. The Journal of infectious diseases. 1998; 177:1660–3. [PubMed: 9607846]
34. Van t Wout JW, Mattie H, van Furth R. Comparison of the efficacies of amphotericin B, fluconazole, and itraconazole against a systemic Candida albicans infection in normal and neutropenic mice. Antimicrobial agents and chemotherapy. 1989; 33:147–51. [PubMed: 2541654]
35. Odds FC, Oris M, Van Dorsselaer P, Van Gerven F. Activities of an intravenous formulation of itraconazole in experimental disseminated Aspergillus, Candida, and Cryptococcus infections. Antimicrobial agents and chemotherapy. 2000; 44:3180–3. [PubMed: 11036047]

36. Kirkpatrick WR, McAtee RK, Fothergill AW, Rinaldi MG, Patterson TF. Efficacy of voriconazole in a guinea pig model of disseminated invasive aspergillosis. Antimicrobial agents and chemotherapy. 2000; 44:2865–8. [PubMed: 10991875]
37. PattersonB, , CoatesP. UK-109,496, a novel, wide-spectrum triazole derivative for the treatment of fungal infections: disposition in man; Program and Abstracts of the 36th Interscience Conference on Antimicrobial Agents and Chemotherapy; New Orleans, Louisiana. 1995;
38. Stevens DA. Animal models in the evaluation of antifungal drugs. J Mycol Med. 1996; 6:7–10.
39. MacCallum DM, Odds FC. Influence of grapefruit juice on itraconazole plasma levels in mice and guinea pigs. The Journal of antimicrobial chemotherapy. 2002; 50:219–24. [PubMed: 12161402]
40. Walsh TJ, Anaissie EJ, Denning DW, Herbrecht R, Kontoyiannis DP, Marr KA, Morrison VA, Segal BH, Steinbach WJ, Stevens DA, van Burik JA, Wingard JR, Patterson TF. Infectious Diseases Society of A. Treatment of aspergillosis: clinical practice guidelines of the Infectious Diseases Society of America. Clinical infectious diseases : an official publication of the Infectious Diseases Society of America. 2008; 46:327–60. [PubMed: 18177225]
41. Sheppard DC, Graybill JR, Najvar LK, Chiang LY, Doedt T, Kirkpatrick WR, Bocanegra R, Vallor AC, Patterson TF, Filler SG. Standardization of an experimental murine model of invasive pulmonary aspergillosis. Antimicrobial agents and chemotherapy. 2006; 50:3501–3. [PubMed: 17005844]
42. Vallor AC, Kirkpatrick WR, Najvar LK, Bocanegra R, Kinney MC, Fothergill AW, Herrera ML, Wickes BL, Graybill JR, Patterson TF. Assessment of Aspergillus fumigatus burden in pulmonary tissue of guinea pigs by quantitative PCR, galactomannan enzyme immunoassay, and quantitative culture. Antimicrobial agents and chemotherapy. 2008; 52:2593–8. [PubMed: 18474582]
43. Sheppard DC, Rieg G, Chiang LY, Filler SG, Edwards JE Jr, Ibrahim AS. Novel inhalational murine model of invasive pulmonary aspergillosis. Antimicrobial agents and chemotherapy. 2004; 48:1908–11. [PubMed: 15105158]
44. Kirkpatrick WR, Najvar LK, Vallor AC, Wiederhold NP, Bocanegra R, Pfeiffer J, Perkins K, Kugler AR, Sweeney TD, Patterson TF. Prophylactic efficacy of single dose pulmonary administration of amphotericin B inhalation powder in a guinea pig model of invasive pulmonary aspergillosis. The Journal of antimicrobial chemotherapy. 2012; 67:970–6. [PubMed: 22240402]
45. UT Health Science Center San Antonio. [Accessed 20 Feb 2016] Invasive Aspergillosis Animal Models Standard Operating ProceduresAvailable from: http://www.sacmm.org/sop.html
46. Boogaerts MA, Maertens J, Van Der Geest R, Bosly A, Michaux JM, Van Hoof A, Cleeren M, Wostenborghs R, De Beule K. Pharmacokinetics and safety of a 7-day administration of intravenous itraconazole followed by a 14-day administration of itraconazole oral solution in patients with hematologic malignancy. Antimicrobial agents and chemotherapy. 2001; 45:981–5. [PubMed: 11181397]
47. Prentice HG, Caillot D, Dupont B, Menichetti F, Schuler U. Oral and intravenous itraconazole for systemic fungal infections in neutropenic haematological patients. Acta Haematol. 1999; 101:56–62. [PubMed: 10085441]
48. Vaughn JM, McConville JT, Burgess D, Peters JI, Johnston KP, Talbert RL, Williams RO III. Single dose and multiple dose studies of itraconazole nanoparticles. European journal of pharmaceutics and biopharmaceutics : official journal of Arbeitsgemeinschaft fur Pharmazeutische Verfahrenstechnik eV. 2006; 63:95–102.
49. Siepmann J, Siepmann F. Mathematical modeling of drug dissolution. International journal of pharmaceutics. 2013; 453:12–24. [PubMed: 23618956]
50. Rabinow B, Kipp J, Papadopoulos P, Wong J, Glosson J, Gass J, Sun CS, Wielgos T, White R, Cook C, Barker K, Wood K. Itraconazole IV nanosuspension enhances efficacy through altered pharmacokinetics in the rat. International journal of pharmaceutics. 2007; 339:251–60. [PubMed: 17398045]
51. Shin JH, Choi KY, Kim YC, Lee MG. Dose-dependent pharmacokinetics of itraconazole after intravenous or oral administration to rats: intestinal first-pass effect. Antimicrobial agents and chemotherapy. 2004; 48:1756–62. [PubMed: 15105131]
52. Hostetler JS, Hanson LH, Stevens DA. Effect of cyclodextrin on the pharmacology of antifungal oral azoles. Antimicrobial agents and chemotherapy. 1992; 36:477–80. [PubMed: 1605615]

53. Warn PA, Sharp A, Mosquera J, Spickermann J, Schmitt-Hoffmann A, Heep M, Denning DW. Comparative in vivo activity of BAL4815, the active component of the prodrug BAL8557, in a neutropenic murine model of disseminated Aspergillus flavus. The Journal of antimicrobial chemotherapy. 2006; 58:1198–207. [PubMed: 17071636]
54. Hoeben BJ, Burgess DS, McConville JT, Najvar LK, Talbert RL, Peters JI, Wiederhold NP, Frei BL, Graybill JR, Bocanegra R, Overhoff KA, Sinswat P, Johnston KP, Williams RO 3rd. In vivo efficacy of aerosolized nanostructured itraconazole formulations for prevention of invasive pulmonary aspergillosis. Antimicrobial agents and chemotherapy. 2006; 50:1552–4. [PubMed: 16569882]
55. Miller JM, Beig A, Carr RA, Spence JK, Dahan A. A win-win solution in oral delivery of lipophilic drugs: supersaturation via amorphous solid dispersions increases apparent solubility without sacrifice of intestinal membrane permeability. Molecular pharmaceutics. 2012; 9:2009–16. [PubMed: 22632106]
56. Yotsuji A, Shimizu K, Araki H, Fujimaki K, Nishida N, Hori R, Annen N, Yamamoto S, Hayakawa H, Imaizumi H, Watanbe Y, Narita H. T-8581, a new orally and parenterally active triazole antifungal agent: in vitro and in vivo evaluations. Antimicrobial agents and chemotherapy. 1997; 41:30–4. [PubMed: 8980750]
57. Sobue S, Sekiguchi K, Nabeshima T. Intracutaneous distributions of fluconazole, itraconazole, and griseofulvin in Guinea pigs and binding to human stratum corneum. Antimicrobial agents and chemotherapy. 2004; 48:216–23. [PubMed: 14693542]
58. Gabardi S, Kubiak DW, Chandraker AK, Tullius SG. Invasive fungal infections and antifungal therapies in solid organ transplant recipients. Transpl Int. 2007; 20:993–1015. [PubMed: 17617181]
59. Collnot EM, Baldes C, Wempe MF, Hyatt J, Navarro L, Edgar KJ, Schaefer UF, Lehr CM. Influence of vitamin E TPGS poly(ethylene glycol) chain length on apical efflux transporters in Caco-2 cell monolayers. Journal of controlled release : official journal of the Controlled Release Society. 2006; 111:35–40. [PubMed: 16410030]
60. Davies B, Morris T. Physiological parameters in laboratory animals and humans. Pharmaceutical research. 1993; 10:1093–5. [PubMed: 8378254]
61. Takashima T, Shingaki T, Katayama Y, Hayashinaka E, Wada Y, Kataoka M, Ozaki D, Doi H, Suzuki M, Ishida S, Hatanaka K, Sugiyama Y, Akai S, Oku N, Yamashita S, Watanabe Y. Dynamic analysis of fluid distribution in the gastrointestinal tract in rats: positron emission tomography imaging after oral administration of nonabsorbable marker, [(18)F]Deoxyfluoropoly(ethylene glycol). Molecular pharmaceutics. 2013; 10:2261–9. [PubMed: 23600944]
62. Brener W, Hendrix TR, McHugh PR. Regulation of the gastric emptying of glucose. Gastroenterology. 1983; 85:76–82. [PubMed: 6852464]
63. Simonian HP, Vo L, Doma S, Fisher RS, Parkman HP. Regional postprandial differences in pH within the stomach and gastroesophageal junction. Digestive diseases and sciences. 2005; 50:2276–85. [PubMed: 16416175]
64. Schiller C, Frohlich CP, Giessmann T, Siegmund W, Monnikes H, Hosten N, Weitschies W. Intestinal fluid volumes and transit of dosage forms as assessed by magnetic resonance imaging. Alimentary pharmacology & therapeutics. 2005; 22:971–9. [PubMed: 16268972]
65. Gotch F, Nadell J, Edelman IS. Gastrointestinal water and electroyltes. IV. The equilibration of deuterium oxide (D2O) in gastrointestinal contents and the proportion of total body water (T.B.W.) in the gastrointestinal tract. J Clin Invest. 1957; 36:289–96. [PubMed: 13406040]

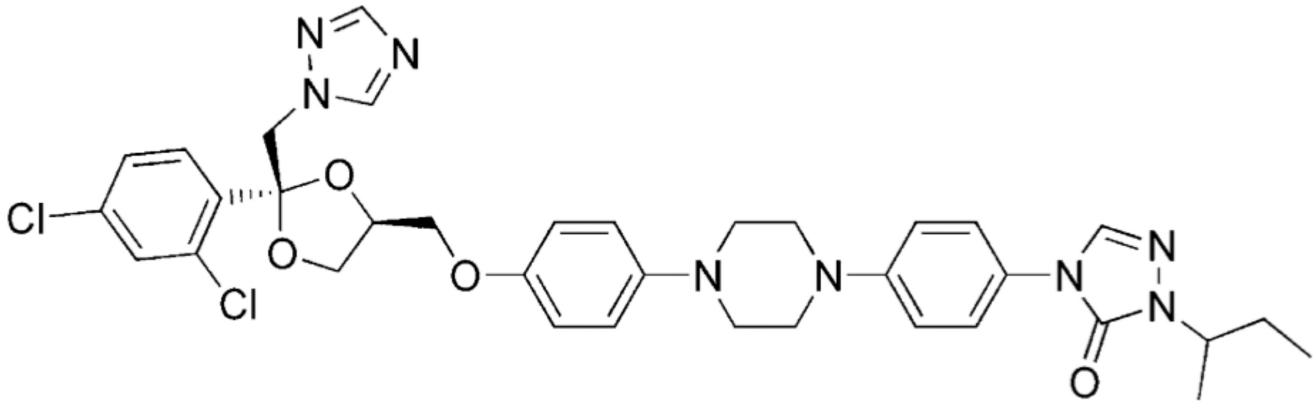

Figure 1.
Chemical structure of itraconazole.

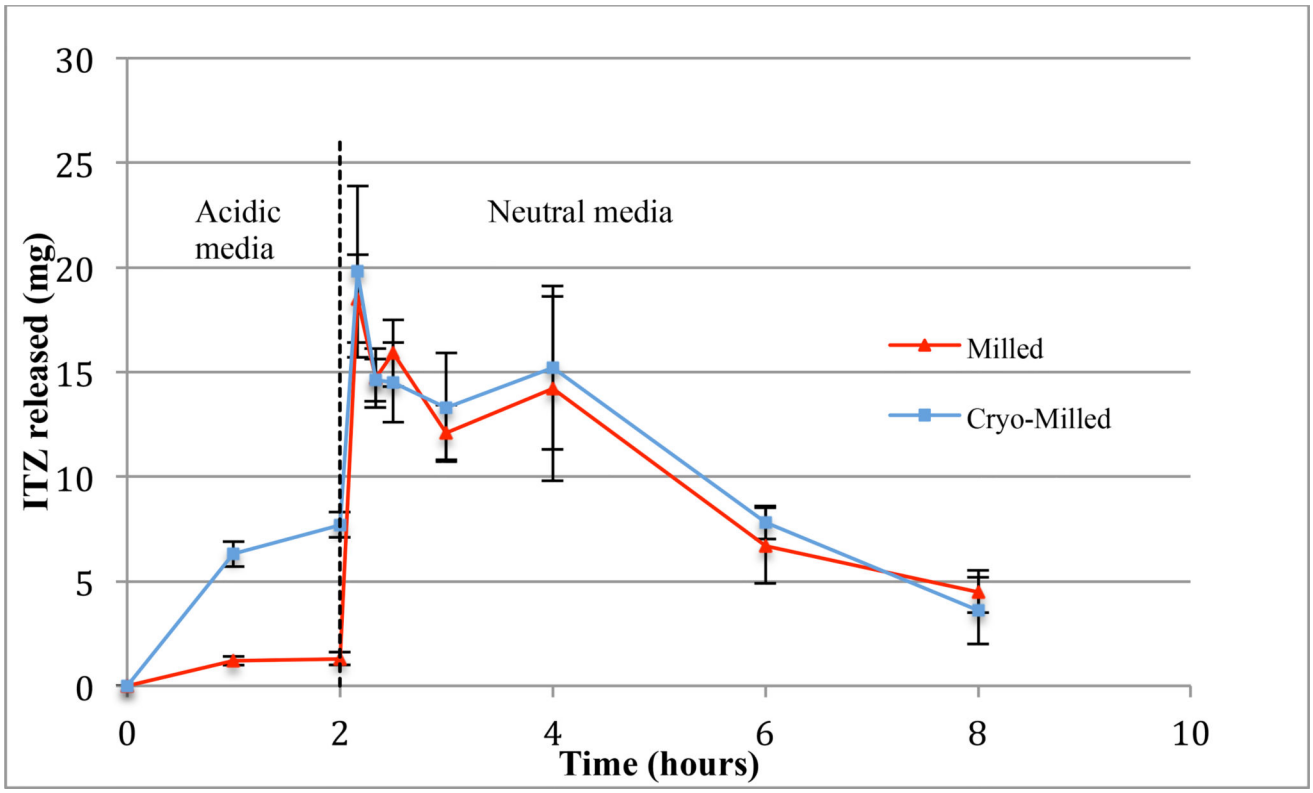

Figure 2.

Supersaturation dissolution testing of HME-ITZ before and after cryo-milling (pH transition conditions). USP 29 apparatus II (paddle), 75 rpm, 37°C. Each dissolution vessel contained the equivalent of 37.5 mg ITZ. Testing was conducted at pH 1.2 followed by transition to pH 6.8 after 2 hours (n =3).

A)

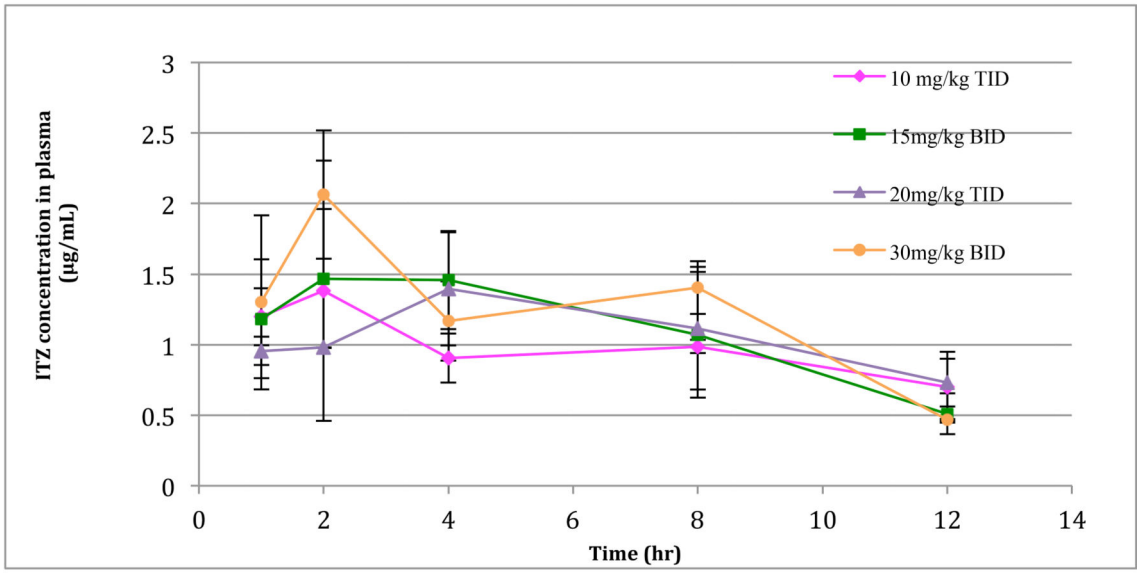

B)

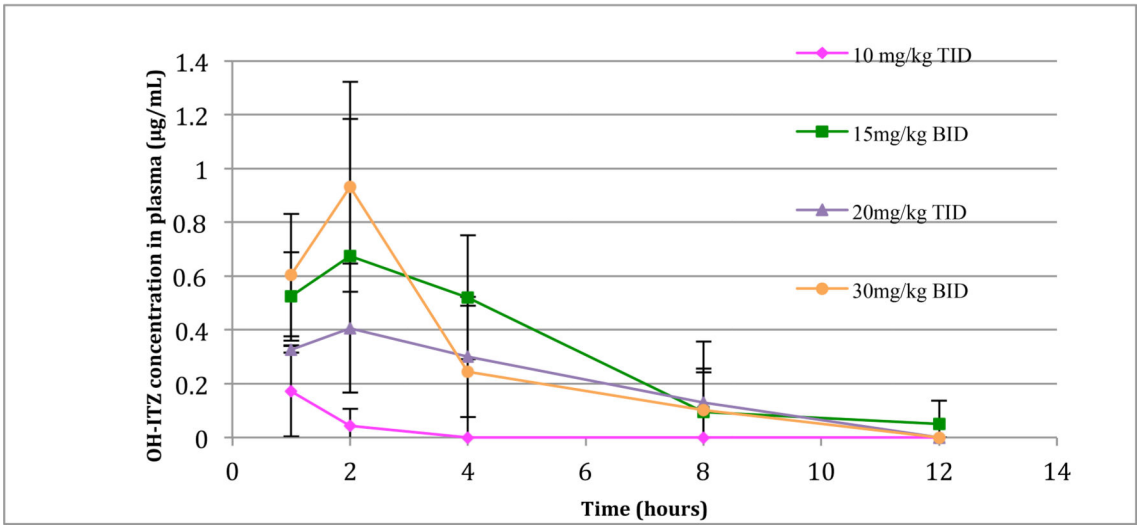

Figure 3.

(A) ITZ and (B) OH-ITZ plasma levels in mice after 7 days of treatment by hot-melt-extrusion processed ITZ (HME-ITZ). Doses were administered by oral gavage in the amount of 10 mg/kg TID, 15 mg/kg BID, 20 mg/kg TID and 30 mg/kg BID per subject (n = 3 ± SD).

(A)

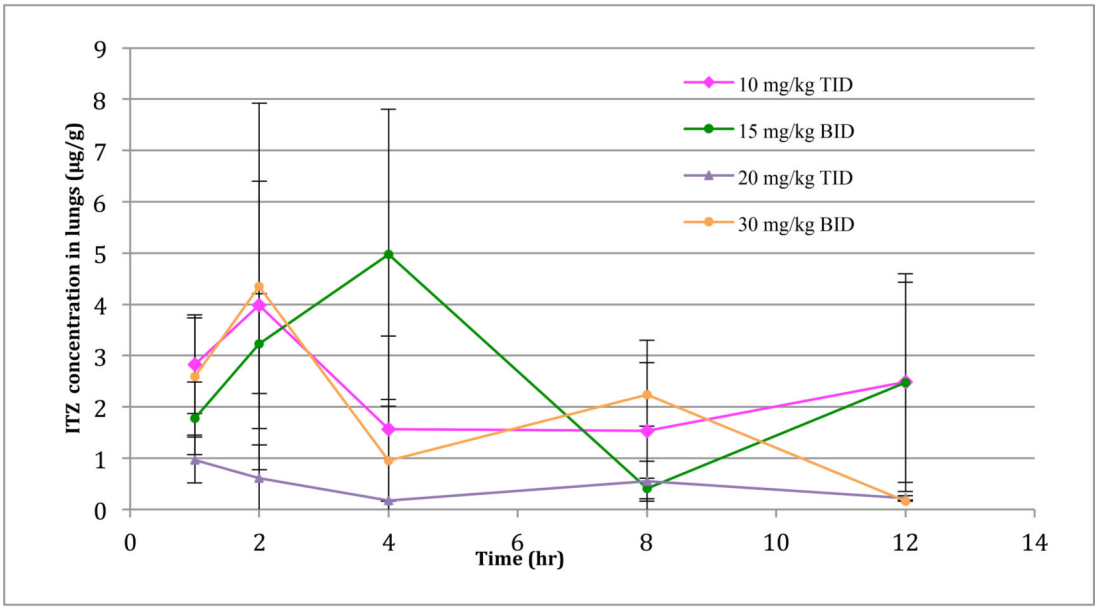

(B)

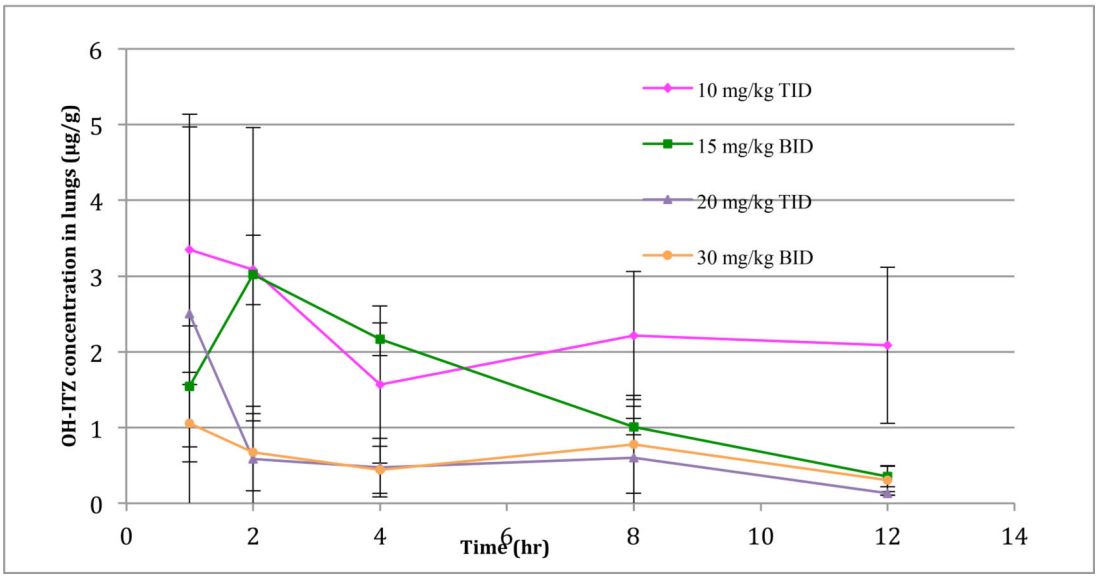

Figure 4.

(A) ITZ and (B) OH-ITZ lungs levels in mice after 7 days of treatment by hot-melt-extrusion processed ITZ (HME-ITZ). Doses were administered by oral gavage in the amount of 10 mg/kg TID, 15 mg/kg BID, 20 mg/kg TID and 30 mg/kg BID per subject (n = 3 ± SD).

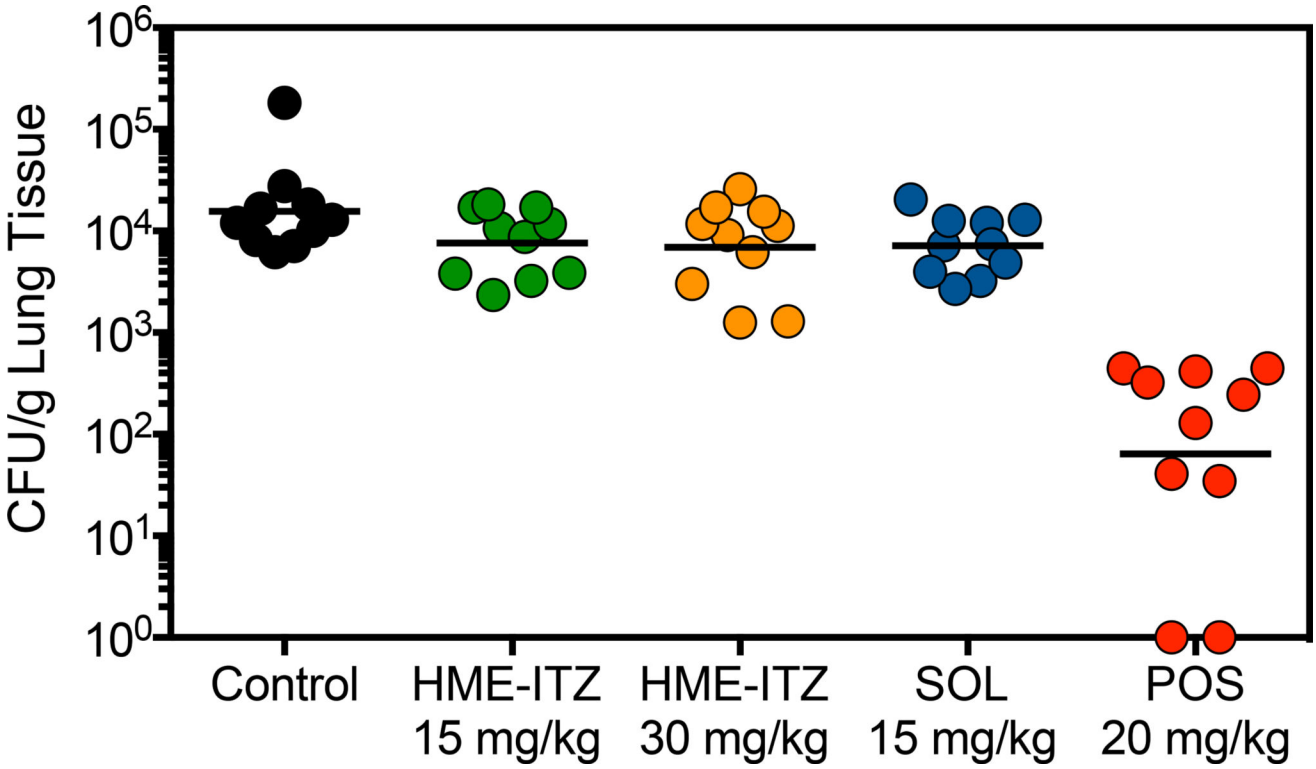

Figure 5.
Pulmonary fungal burden at day 8 in mice treated by HME-ITZ, ITZ cyclodextrin solution and posaconazole (n=10). Pulmonary fungal burden is given in terms of Aspergillus fumigatus DNA concentration measured by colony forming units.

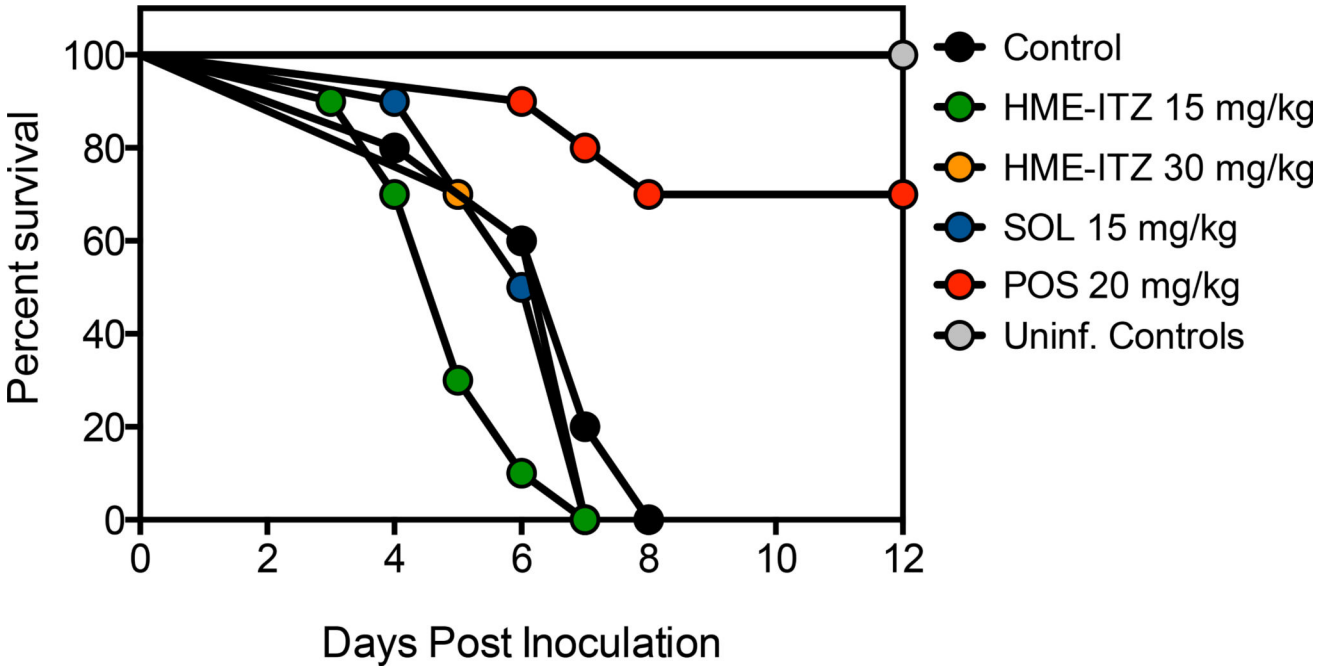

Figure 6.

Survival curves in mice treated by hot-melt-extrusion processed ITZ (HME-ITZ), ITZ cyclodextrin solution (SOL) and posaconazole (POS). Therapy was administered during 7 days and mice were followed off therapy until day 12 (n=10).

A)

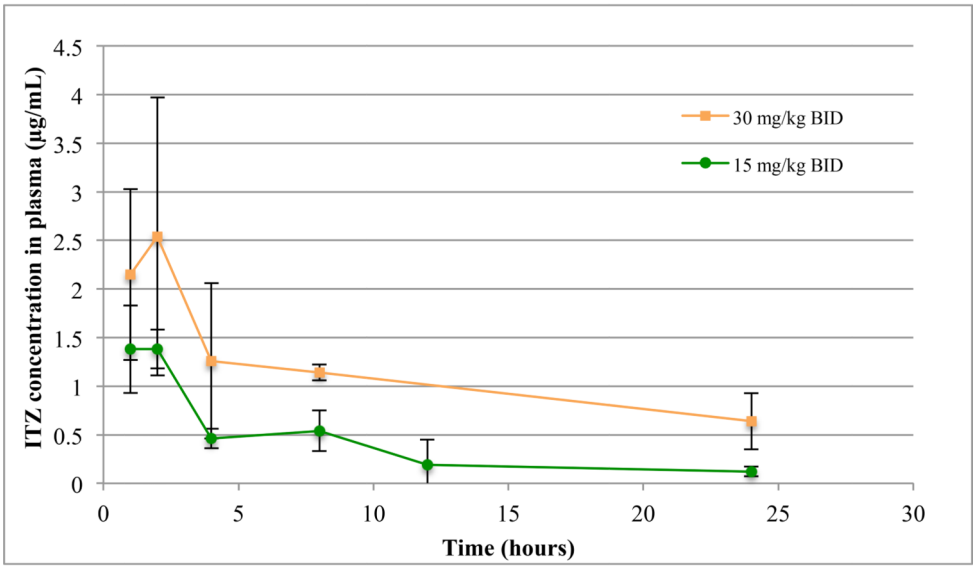

B)

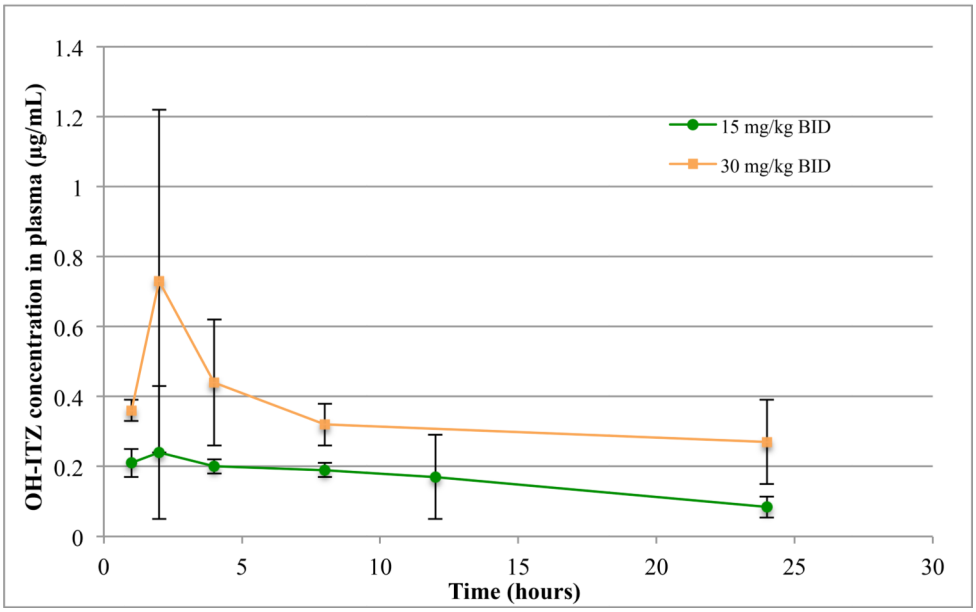

Figure 7.

(A) ITZ and (B) OH-ITZ plasma levels in guinea pig after 7 days of treatment by hot-melt-extrusion processed ITZ (HME-ITZ). Doses were administered by oral gavage in the amount of 15 mg/kg BID and 30 mg/kg BID (n = 3 ± SD).

A)

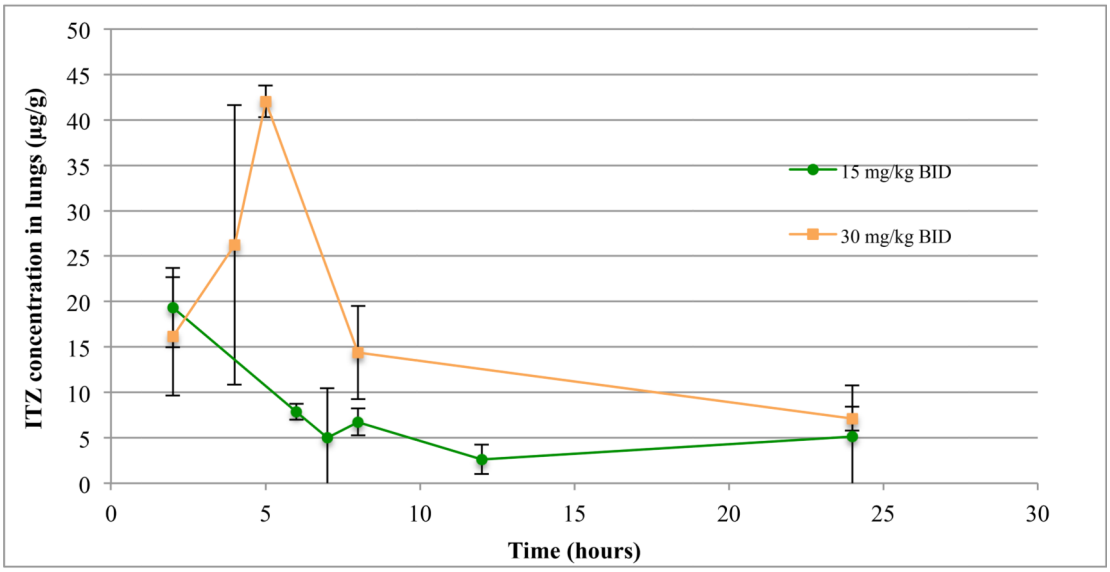

B)

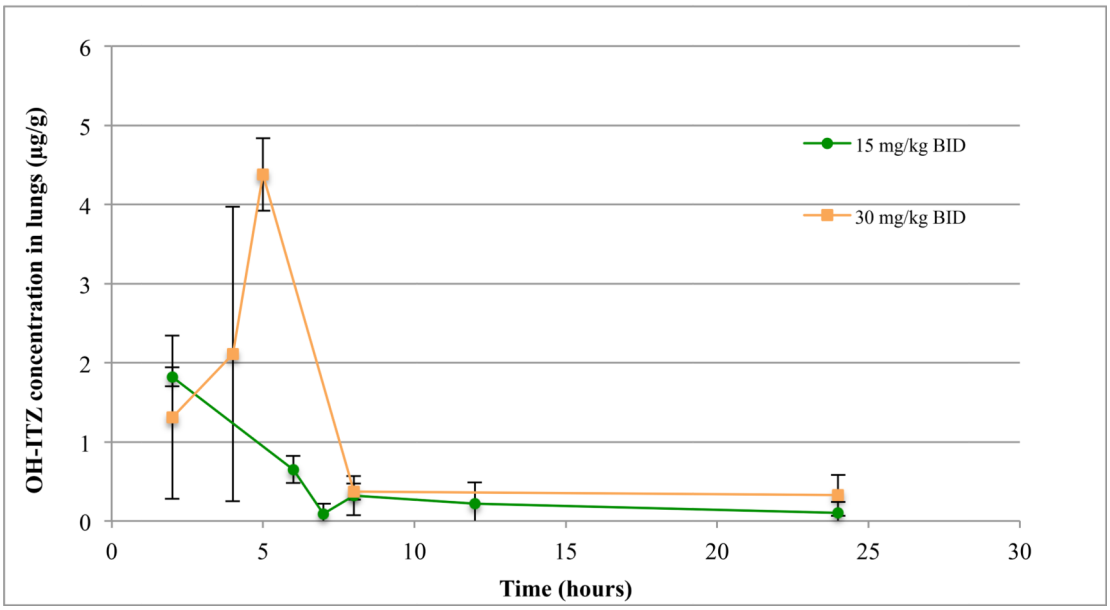

Figure 8.

(A) ITZ and (B) OH-ITZ lung levels in guinea pig after 7 days of treatment by hot-melt-extrusion processed ITZ (HME-ITZ). Doses were administered by oral gavage in the amount of 15 mg/kg BID and 30 mg/kg BID (n = 3 ± SD).

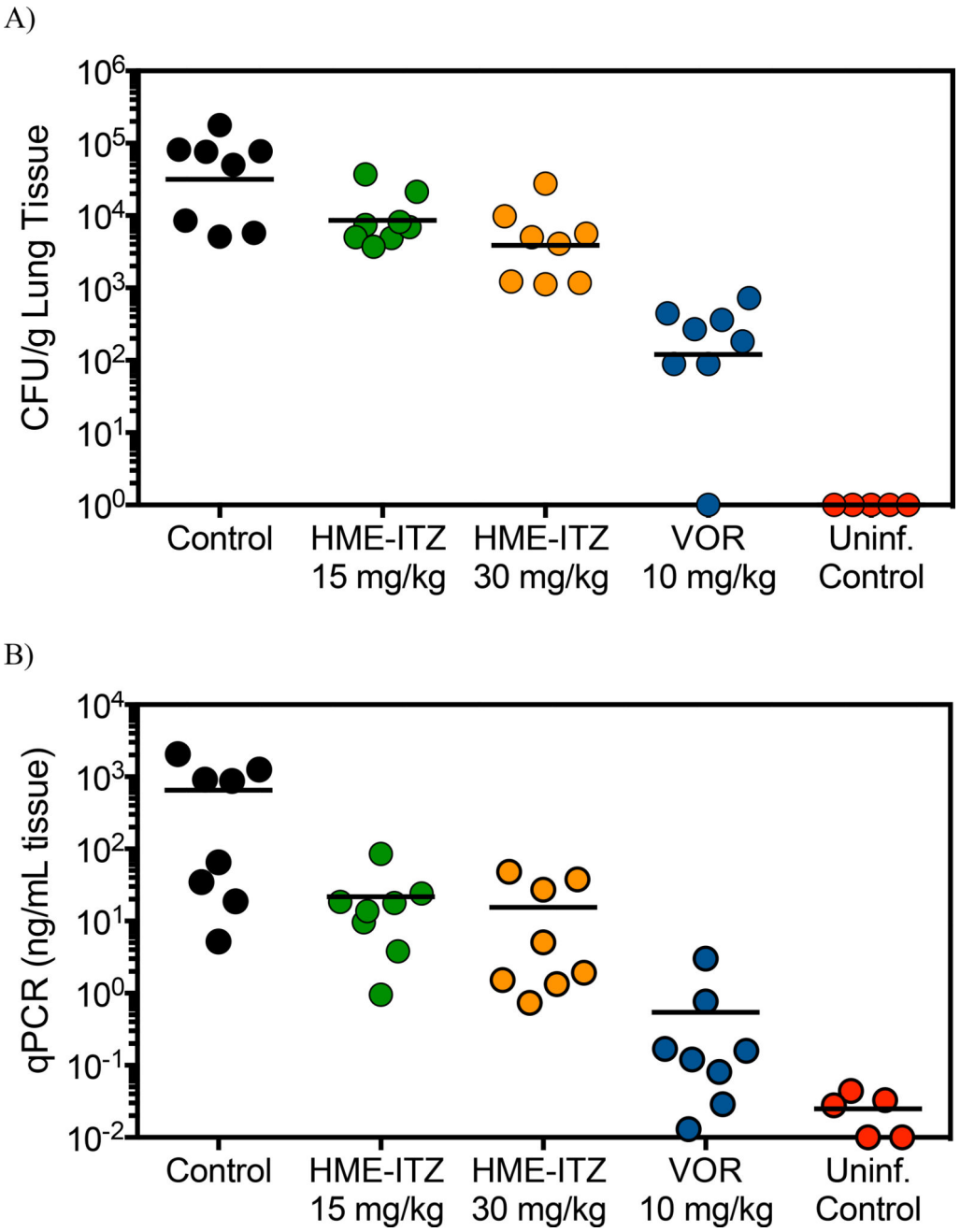

Figure 9.

Pulmonary fungal burden at day 8 in guinea pigs treated by HME-ITZ and voriconazole (VOR) as compared to untreated animals (infected and uninfected) (n=8). Pulmonary fungal burden is given in terms of (A) *Aspergillus fumigatus* CFUs and (B) *Aspergillus fumigatus* DNA concentration measured by real time quantitative PCR.

Table 1

Area Under the Dissolution Curve (AUDC) Values for pH transition dissolution testing of HME-ITZ before and after cryo-milling.

Formulation	$AUDC_{acid}$ (mg.min)	$AUDC_{neutral}$ (mg.min)	$AUDC_{total}$ (mg.min)
HME-ITZ Milled	113.4 ± 10.0	3,559.6 ± 80.9	3,673.0 ± 65.2
HME-ITZ Cryo-milled	608.7 ± 27.0	3,786.8 ±103.5	4,395.5 ± 84.1

Table 2

Pharmacokinetic data (C_{max} and $AUC_{t0–8h}$)in lungs and plasma of mice and guinea pigs after different dosing schedules following the dose tolerability study.

	ITZ in mice Lungs				ITZ in guinea pigs lungs	
	10 mg/kg TID	15 mg/kg BID	20 mg/kg TID	30 mg/kg BID	15 mg/kg BID	30 mg/kg BID
Cmax (μg/g)	3.99 ± 2.41	4.98 ± 2.83	0.96 ± 0.44	4.34 ± 3.58	19.35 ± 4.38	42.02 ± 1.74
$AUC_{t0–8h}$ (μg.h/g)	16.63±0.43	22.36 ± 2.26	3.04 ± 0.39	15.26 ± 2.05	77.68 ± 1.73	148.84 ± 13.01
	ITZ in mice plasma				ITZ in guinea pigs plasma	
Cmax (μg/mL)	1.38 ± 0.92	1.47 ± 0.49	1.39 ± 0.40	2.06 ± 0.45	1.38 ± 0.21	2.54 ± 1.43
$AUC_{t0–8h}$ (μg.h/mL)	7.95 ± 0.47	9.90 ± 0.50	8.82 ± 0.99	10.55 ± 0.44	5.92 ± 0.28	12.94 ± 1.28

Table 3

ITZ and OH-ITZ concentrations in mice and guinea pig tissues on day 8 following the efficacy study (n=8).

		ITZ conc.	OH-ITZ conc.
Mice - Plasma	15 mg/kg BID	n.d	n.d
	30 mg/kg BID	n.d	n.d
Guinea Pig - Plasma	15 mg/kg BID	1.04 ± 0.83 µg/mL	0.23 ± 0.31 µg/mL
	30 mg/kg BID	2.49 ± 0.91 µg/mL	0.91 ± 0.40 µg/mL
Guinea Pig - Brain	15 mg/kg BID	2.59 ± 1.85 µg/g	0.08 ± 0.059 µg/g
	30 mg/kg BID	9.39 ± 3.43 µg/g	0.57 ± 0.32 µg/g

n.d : not detectable

Table 4

Mice, guinea pigs, rats and human gastro-intestinal tract characteristics

	Mice[31]	Guinea Pig[32]	Rats[31, 60, 61]	Human[62, 63, 64, 65]
Stomach pH fasted	4.0	n.a	4 – 5	1 – 3.5
Stomach pH fed	3.0	2.9	6.5 – 7.1	3.0 – 6.0
Stomach water volumes	0.37 – 0.71 g	~ 15 g	~ 2.4 g	~ 118 g
Stomach capacity	0.4 mL	n.a	3.4 mL	n.a
Intestine pH fasted	5.0	n.a	4.5 – 7.5	5.5 – 8
Intestine pH fed	4.8	6.0 – 7.4	5.0 – 7.1	5.0 – 6.5
Intestinal water volumes	0.6 – 0.8 g	~ 38 g	3.0 – 4.6 g	~ 206 g
Intestinal tract length	32–54 cm	236 – 260 cm	82 – 115 cm	~ 8.6 m